Chirp and Compress: Toward Single-Cycle Biphotons

S. E. Harris*

Edward L. Ginzton Laboratory, Stanford University, Stanford, California 94305, USA

(Received 5 August 2006; published 5 February 2007)

The Letter describes a technique for the spontaneous generation of chirped time-energy entangled photons. Transmitting either photon through an appropriate dispersive medium results in a temporally compressed, transform limited biphoton. At maximum bandwidth, the biphoton is a single cycle in length, with a waveform that has the same characteristic shape as a classical single-cycle pulse.

DOI: 10.1103/PhysRevLett.98.063602 PACS numbers: 42.50.Dv, 42.50.Ct, 42.65.Re

When the bandwidth of an optical pulse is equal to, or greater than, its central frequency and when all of its spectral components are in phase, the pulse develops a characteristic waveform that is termed as single cycle [1,2]. In this Letter, we describe a technique for generating nonclassical pairs of photons (biphotons) whose characteristic coincidence time, as measured at distant detectors, is a single optical cycle. The elements of the technique are (1) the suggestion for using parametric down conversion to spontaneously generate pairs of entangled photons whose instantaneous frequencies are chirped in opposite directions, and (2) the use of the nonlocal nature of entangled photons [3] to allow the dispersion, as experienced by one photon, to cancel out the dispersion of the second photon and to compress the biphoton wave packet.

A key motivation for the study of single-cycle biphotons is their potential application to nonlinear optical processes with nonclassical fields [4]. Here we follow Silberberg and use sum frequency generation as an ultrafast correlator [5]. As shown below, the efficiency for generating sum frequency photons varies inversely with the width of the incoming biphoton; i.e., single-cycle biphotons behave as if they have an effective power equal to their energy divided by their temporal width. Similarly, in the absence of intermediate resonances, single-cycle biphotons maximize the two photon transition probability. Other uses for ultra-wideband biphotons include nonclassical metrology [6] and large bandwidth quantum information processing [7,8].

As shown in Fig. 1, we make use of a quasi-phase-matched (QPM) periodically poled crystal [9]. The up-down arrows show the direction of the $\bar{a}_z$ axis of the domains of the crystal. These domains are reversed with a period Λ such that the corresponding spatial frequency, $2\pi/\Lambda$, is linearly chirped. The poling period is chosen so that the signal frequency is phase matched for red emission at the left end of the crystal and for blue emission at the right end of the crystal. Paired photons that are emitted from the right end arrive at their respective photodetectors at the same time. Paired photons that are emitted from the left end of the crystal arrive at the photodetector with a time difference determined by their group velocities. In the ideal case where there is no group velocity dispersion, the biphoton wave packet is (exactly) linearly chirped.

Figure 2 shows the near-white light spectrum of a 2 cm long QPM crystal of $LiNbO_3$ pumped with a monochromatic laser at a wavelength of 0.42 μm. Here, the spatial frequency of the domain reversals varies linearly with distance and is chosen so that the crystal is phase matched at a wavelength of 0.750 μm at the left end and at a wavelength of 0.464 μm at the right end. This corresponds to a poling period of 3.11 μm at the left end and 7.02 μm at the right end of the crystal. When compressed, this spectrum corresponds to a biphoton with a temporal length that is nearly a single optical cycle at the degenerate wavelength of 0.84 μm. The refractive index as a function of frequency, for this and other figures, is $n_e(\omega)$ and is obtained from the Sellmeier equation for $\bar{a}_z$ polarized light in $LiNbO_3$ [10].

Before proceeding, we note further pertinent work: Torner and Teich and colleagues have suggested the use of a chirped QPM crystal to broaden the bandwidth and to thereby improve the resolution of optical coherence tomography [11]. Shih and colleagues have shown how a dispersive medium will broaden a biphoton wave packet and have suggested the use of compensation [12,13]. In a series of beautiful experiments, Silberberg and his colleagues have demonstrated control of the temporal shapes of down-converted photons and the use of frequency summing as an ultrafast correlator [5,14,15].

We take the spatial frequency of the QPM crystal as $K_0 - \zeta z$ where K_0 is chosen to phase match the crystal at a

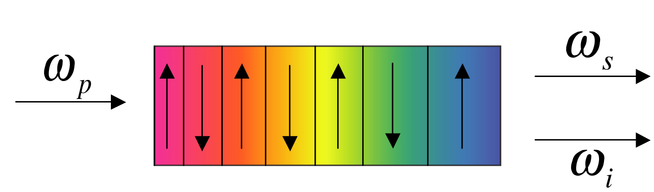

FIG. 1 (color online). Quasi-Phase-Matching. The up-down arrows show the direction of the $\bar{a}_z$ axis of the domains of the quasi-phase-matched crystal. The poling period is chosen so that the signal frequency is phase matched for red emission at the left end of the crystal and for blue emission at the right end of the crystal.

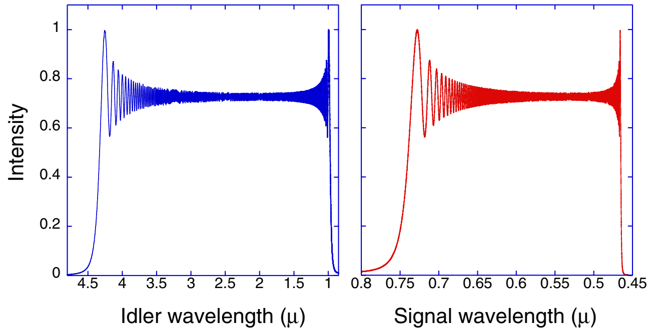

FIG. 2 (color online). Calculated spectrum of spontaneously generated chirped photons for a 2 cm long QPM crystal of $LiNbO_3$ pumped at 0.42 μm.

selected frequency at its left end, and ζ is chosen to phase match a selected frequency at its right end. The functional form of the spatially varying nonlinearity is $\exp(i\int_0^z \zeta z dz) = \exp(i\zeta z^2/2)$. We assume a monochromatic pump at ω_p and take the signal and idler frequencies as $\omega_s = \omega$ and $\omega_i = \omega_p - \omega$. Both the signal and idler frequencies are positive, with the signal frequency defined to be in the range $\omega_p/2 \leq \omega \leq \omega_p$.

Time domain signal and idler operators are related to their frequency domain counterparts by $a_s(t, z) = \int_{-\infty}^{\infty} a_s(\omega, z)\exp(-i\omega t)d\omega$ and $a_i(t, z) = \int_{-\infty}^{\infty} a_i(\omega_i, z) \times \exp[-i(\omega_p - \omega)t]d\omega$. We introduce operators $b(\omega, z)$ that vary slowly with distance, as compared to a wavelength, by letting $a(\omega, z) = b(\omega, z)\exp[ik(\omega)z]$. The coupled equations for the operators $b_s(\omega_s, z)$ and $b_i^\dagger(\omega_i, z)$ are

$$\frac{\partial b_s}{\partial z} = i\kappa b_i^\dagger \exp\left(i\frac{\zeta z^2}{2}\right)\exp[i\Delta k(\omega)z]$$
$$\frac{\partial b_i^\dagger}{\partial z} = -i\kappa^* b_s \exp\left(-i\frac{\zeta z^2}{2}\right)\exp[-i\Delta k(\omega)z]. \quad (1)$$

The quantity $\Delta k(\omega) = k_p(\omega_p) - [k_s(\omega) + k_i(\omega_i) + K_0]$, where $k(\omega) = \omega n(\omega)/c$. Dispersion, to all orders, is included in Eq. (1), and there is no assumption requiring that the temporal variation be slow.

We solve Eq. (1) by the same method that one would use to solve similar classical equations: We assume that the parametric gain is small and replace the quantities $b_s(z)$ and $b_i^\dagger(z)$ by their values at $z = 0$, i.e., let $b_s(z) = b_s(0)$ and $b_i^\dagger(z) = b_i^\dagger(0)$. Equation (1) may then be integrated over the crystal length L. The quantities $a_s(\omega, L)$, and $a_i^\dagger(\omega_i, L)$ may be written as

$$a_s(\omega, L) = A_1(\omega)a_s(\omega, 0) + B_1(\omega)a_i^\dagger(\omega_i, 0)$$
$$a_i^\dagger(\omega_i, L) = C_1(\omega)a_s(\omega, 0) + D_1(\omega)a_i^\dagger(\omega_i, 0), \quad (2)$$

where $A_1(\omega) = \exp[ik_s(\omega)L]$, $D_1(\omega) = \exp[-ik_i(\omega_i)L]$, $C_1(\omega) = B_1^*(\omega)\exp[i(k_s(\omega) - k_i(\omega_i))L]$, and

$$B_1(\omega) = -(-1)^{1/4}\left(\frac{\pi}{2\zeta}\right)^{1/2}\kappa\exp[ik_s(\omega)L] \times \exp\left[\frac{-i\Delta k(\omega)^2}{2\zeta}\right]\left\{\mathrm{erfi}\left[\frac{(1+i)\Delta k(\omega)}{2\sqrt{\zeta}}\right] - \mathrm{erfi}\left[\frac{(1+i)(\Delta k(\omega) + \zeta L)}{2\sqrt{\zeta}}\right]\right\}. \quad (3)$$

where erfi is the imaginary error function.

The spectral power density at the signal is $S(\omega) = \int \langle 0|a_s^\dagger(\omega_1)a_s(\omega_2)|0\rangle \exp[-i(\omega_2 - \omega_1)t]d\omega_2$. Noting the commutator, $[a_j(\omega_1, 0), a_k^\dagger(\omega_2, 0)] = \frac{1}{2\pi}\delta_{jk}\delta(\omega_1 - \omega_2)$,

$$S(\omega) = \frac{1}{2\pi}|B_1(\omega)|^2. \quad (4)$$

The total paired count rate is $R = \int_{\omega_p/2}^{\omega_p} S(\omega)d\omega$ and is independent of the chirping parameter ζ. For the 2 cm crystal of $LiNbO_3$ pumped by a confocally focused 1 W laser at 0.42 μm, the integrated count rate for the spectrum of Fig. 2 is 1.3×10^{10} pairs s^{-1}.

From the functional form of $B_1(\omega)$, we deduce that to attain bandwidth limited compression of the chirped biphoton, we should place an optical element in the path of the signal beam whose transfer function is

$$H(\omega) = \exp\left[i\left(\frac{\Delta k(\omega)^2}{2\zeta} - q(\omega)\right)\right], \quad (5)$$

where $q(\omega) = [k_s(\omega) + k_i(\omega_p - \omega)]L$. The effect of this transfer function is to cause the paired signal and idler photons, irrespective of their frequencies, to arrive at distant detectors (or at the summing crystal) at the same time. Though neither the signal or the idler photon is itself transform limited, the biphoton is.

An example is the case of a signal and idler that are phase matched at center frequencies ω_{so} and ω_{io} and have a bandwidth that is sufficiently small that biphoton compression may be accomplished using quadratic dispersion. With $\delta\omega = \omega - \omega_{so}$, $\Delta k(\delta\omega)$ is approximated as $\Delta k(\delta\omega) = (1/V_s - 1/V_i)\delta\omega = (1/V_r)\delta\omega$, where V_s and V_i are the signal and idler group velocities at their center frequencies and V_r is the relative group velocity. The transfer function of the compensating element becomes $H(\omega) = \exp[i\delta\omega^2/(2V_r^2\zeta)]\exp[i\delta\omega L/V_r]$. For a crystal of length L, the bandwidth of the chirped source is $BW = \zeta V_r L$, the group delay is $\tau_D = L/V_r$, and $H(\omega) = \exp[i(\tau_D\delta\omega^2)/(2BW)]\exp[i\delta\omega L/V_r]$. This is the well-known function for quadratic compression and delay of a smooth chirped classical pulse.

We make use of sum frequency generation as an ultrafast correlator [15]. In Fig. 3(a), signal and idler photons sum to regenerate monochromatic photons at the pump frequency ω_p. Because the signal and idler photons arrive at the summing crystal simultaneously, the rate of generated sum frequency photons varies linearly, rather than as the square, of the rate R of incoming paired photons [4]. By

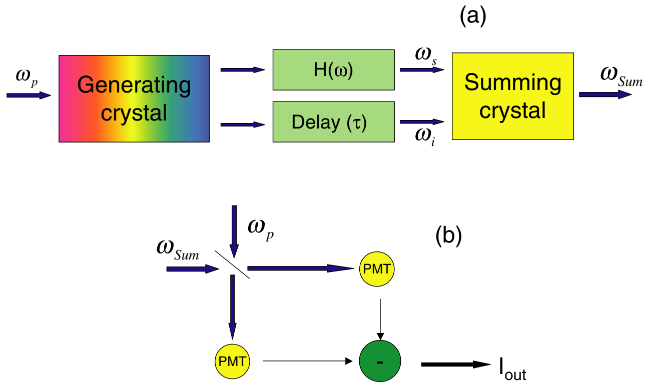

FIG. 3 (color online). (a) Frequency Summing as an ultrafast correlator. Signal and idler photons sum to produce monochromatic photons at frequency ω_p. The envelope of the biphoton wave function is obtained by varying the time delay τ. (b) Homodyning the generated sum frequency with the pump beam and varying the time delay τ yield the biphoton wave function.

measuring the average power at the sum frequency as a function of the time delay τ between the signal and idler photons, we measure the envelope of the biphoton wave function.

To write the expression for the generated sum power, we replace the coefficients in Eq. (3) with coefficients that include the dispersion compensating function $H(\omega)$ in the signal channel and a time delay function $G(\omega, \tau) = \exp[-i(\omega_p - \omega)\tau]$ in the idler channel. These are $A(\omega) = H(\omega)A_1(\omega)$, $B(\omega) = H(\omega)B_1(\omega)$, $C(\omega, \tau) = G(\omega, \tau)C_1(\omega)$, and $D(\omega, \tau) = G(\omega, \tau)D_1(\omega)$.

The rate of generated sum photons is

$$R_{\mathrm{sum}}(\tau) = \eta_1\left[R^2 + \left|\left(\frac{1}{2\pi}\right)\int_{\omega_p/2}^{\omega_p} A(\omega)C^*(\omega, \tau)d\omega\right|^2\right]. \tag{6}$$

The first term in Eq. (6) is the same as its classical equivalent where the output power depends on the square of the input power, and the efficiency factor η_1 is equal to its classical value. The second term is equal to the square of the amplitude of the biphoton wave function. For a wave function of width T_p, the ratio of the peak height of the second term to the first is approximately $1/(RT_p)$. Equation (6) has the same form as the Glauber intensity correlation function [16]. In a summing experiment of this type, but near degeneracy [5], Silberberg and colleagues report an estimated count rate at the sum frequency of 40 000 counts/s. Here, because the bandwidths will be much broader, to allow phase matching, the summing crystal must be very thin, and we anticipate about 100 counts/s.

The technique of the previous paragraph measures the envelope, or equivalently, the correlation time of the biphoton wave packet. To measure the waveform itself, for example, a frequency chirp, we require a reference phase. As shown in Fig. 3(b), we obtain this phase by homodyning the generated sum frequency against the original monochromatic pumping laser, and as before, varying the path length of the idler beam τ. The output current of the balanced homodyne detector is calculated as

$$I_{\mathrm{out}} = \left(\frac{1}{2\pi}\right)\Re\left[\int_{\omega_p/2}^{\omega_p} e^{i\phi}A(\omega)C^*(\omega)d\omega\right]. \tag{7}$$

Here, ϕ is the phase of the local oscillator with respect to the original pumping beam.

We illustrate the measurement technique by applying it to a chirped waveform that is generated in an ideal medium where there is no group velocity dispersion. Figure 4 shows the waveform (solid line) and its envelope (dashed line) for a red to blue chirped biphoton with about one octave of signal bandwidth. Here, in order to make the chirp apparent, we assume a low enough pump frequency that there are a limited number of cycles beneath the waveform envelope. Signal and idler photons sum to monochromatic photons at the pump frequency. As in classical nonlinear optics, the phase of the generated sum field varies with the phase of the input fields. Homodyne detection resolves this phase and allows cycle-by-cycle measurement of the relative frequency of the signal and idler. A linear chirp, in correspondence with the chirping parameter ζ, is obtained.

Figure 5 shows an example of the chirp and compress technique for $LiNbO_3$ with a small chirp and quadratic compression. For comparison, Fig. 5(a) shows sum power, normalized to the classically generated power, for a uniformly poled (nonchirped) crystal of length of 2 cm and relative group velocity V_r. The width of the envelope of the

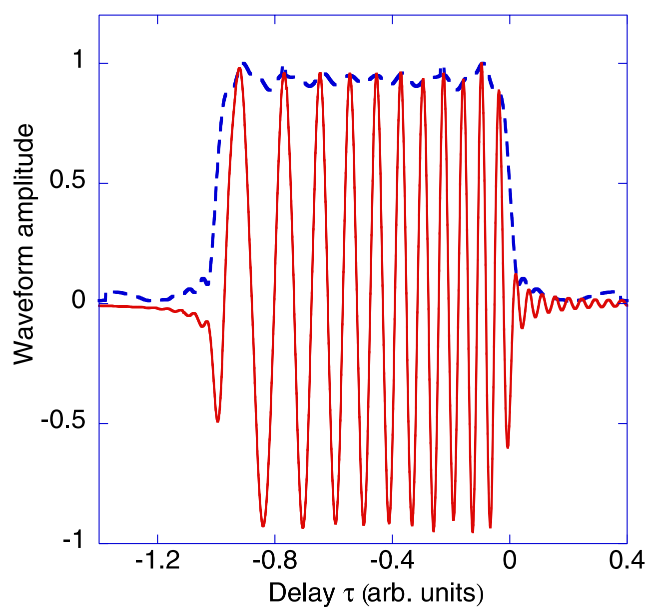

FIG. 4 (color online). Chirped biphoton waveform and its envelope.

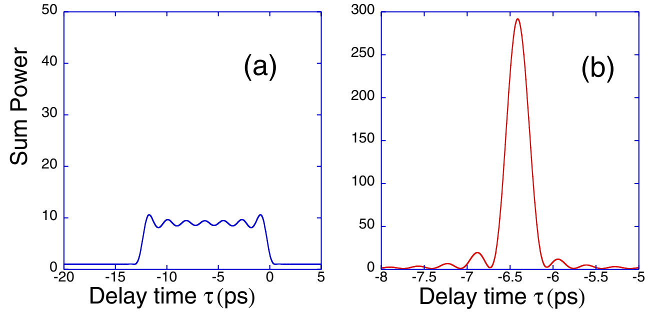

FIG. 5 (color online). Calculated normalized sum power as a function of delay. (a) The QPM crystal is uniformly poled to phase match at 0.6 μm with a bandwidth of 2.6 cm^{-1}. (b) The poling period is chirped to produce a bandwidth of 122 cm^{-1}, and the wave packet is quadratically compressed.

biphoton wave function is L/V_r [17] and is 12.6 ps, and the linewidth is 2.6 cm^{-1}. For Fig. 5(b), the poling period is chirped with parameter $\zeta = 6.01 \times 10^5$ to produce a bandwidth of 122 cm^{-1} and the function $H(\omega) = \exp[i\delta\omega^2/(2V_r^2\zeta)]$. The width of the biphoton wave packet is reduced, and the sum power is increased, both by a factor of about 30.

Figure 6(a) assumes a very large chirp that produces the spectrum of Fig. 2. Here, we assume ideal compression using $H(\omega)$ of Eq. (5). The pulse is now compressed to a length of 3.6 fs, or about 1.3 cycles at the degenerate wavelength of 0.84 μm, and the peak sum frequency power is increased by a factor of over a thousand.

Figure 6(b) shows the output current obtained by the homodyne technique of Fig. 3 as a function of the delay time τ in the idler channel. We observe a single-cycle waveform that is nominally the same as a classical pulse with one octave of bandwidth. Of interest, the (adjustable) phase of the local oscillator relative to the pump plays the role of the carrier-envelope phase of a classical waveform. As this phase is varied (not shown), one sweeps through the locus of single-cycle waveforms.

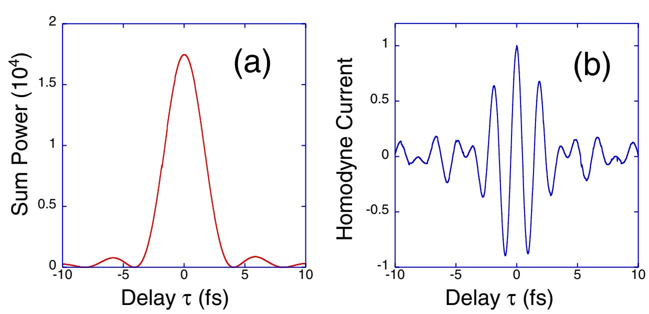

FIG. 6 (color online). (a) Normalized sum power and (b) homodyne current for a single-cycle pulse in $LiNbO_3$. Dispersion is corrected as per Eq. (5).

The author thanks Sunil Goda, Pavel Kolchin, Steve Sensarn, and Edo Waks for helpful discussions. This work was supported by the U.S. Air Force Office of Scientific Research, the U.S. Army Research Office, and the Defense Advanced Research Projects Agency.

*Electronic address: seharris@stanford.edu

[1] D. You and P. H. Bucksbaum, J. Opt. Soc. Am. B **14**, 1651 (1997).
[2] M. Y. Shverdin, D. R. Walker, D. D. Yavuz, G. Y. Yin, and S. E. Harris, Phys. Rev. Lett. **94**, 033904 (2005).
[3] J. D. Franson, Phys. Rev. A **45**, 3126 (1992).
[4] J. Gea-Banacloche, Phys. Rev. Lett. **62**, 1603 (1989); N. Ph. Georgiades, E. S. Polzik, K. Edamatsu, H. J. Kimble, and A. S. Parkins, Phys. Rev. Lett. **75**, 3426 (1995).
[5] B. Dayan, A. Pe'er, A. A. Friesem, and Y. Silberberg, Phys. Rev. Lett. **94**, 043602 (2005).
[6] V. Giovannetti, S. Lloyd, and L. Maccone, Phys. Rev. Lett. **96**, 010401 (2006).
[7] I. A. Khan and J. C. Howell, Phys. Rev. A **73**, 031801(R) (2006).
[8] C. K. Law, I. A. Walmsley, and J. H. Eberly, Phys. Rev. Lett. **84**, 5304 (2000).
[9] L. E. Myers, R. C. Eckardt, M. M. Fejer, R. L. Byer, W. R. Bosenberg, and J. W. Pierce,J. Opt. Soc. Am. B **12**, 2102 (1995).
[10] The refractive index for $LiNbO_3$ as a function of frequency is $n_e(\omega)$, as obtained from Casix, Inc.
[11] S. Carrasco, J. P. Torres, L. Torner, A. Sergienko, B. Saleh, and M. Teich, Opt. Lett. **29**, 2429 (2004).
[12] A. Valencia, M. V. Chekhova, A. Trifonov, and Y. Shih, Phys. Rev. Lett. **88**, 183601 (2002).
[13] Y. Shih, Rep. Prog. Phys. **66**, 1009 (2003).
[14] B. Dayan, A. Pe'er, A. A. Friesem, and Y. Silberberg, Phys. Rev. Lett. **93**, 023005 (2004).
[15] A. Pe'er, B. Dayan, A. A. Friesem, and Y. Silberberg, Phys. Rev. Lett. **94**, 073601 (2005).
[16] P. Kolchin, "EIT Based Paired Photon Generation" (to be published).
[17] M. H. Rubin, D. N. Klyshko, Y. H. Shih, and A. V. Sergienko, Phys. Rev. A **50**, 5122 (1994).